Final Report on Contract F61775-00-We 054 Submitted to the European Office of Aerospace Research and Development (EOARD)

Deflagration to Detonation Transition Processes in Pulsed Detonation Engines

Organization Imperial College Consultants Limited, 47 Prince's Gate, Exhibition Road, London SW7 2QA, UK

Type of Organisation A firm of consultants wholly owned by Imperial College.

Principal Investigator Prof. R.P. Lindstedt
Contact Details Imperial College of Science, Technology and Medicine, Department of Mechanical Engineering Exhibition Road, London SW7 2BX, UK. email p.lindstedt@ic.ac.uk; telephone 020 – 75947039; fax 020 – 7594 7243.

Summary

The aim of the work performed in the current contract is to assess the accuracy of potential modelling techniques applied to the formation of Deflagration to Detonation (DDT) kernels in mixtures of hydrocarbons with air. The application area is of direct relevance to the transition to detonation in pulsed detonation engines featuring premixed gases. The latter technology is currently pursued at Wright Laboratories and the current evaluation is directly linked to this technology. Key aspects covered include guidance on suitable theoretical development directions and a preliminary investigation of optimal conditions for transition to detonation. The work is technically demanding and features several aspects that has not previously been accomplished. The main conclusions of the study are perhaps surprisingly positive. The work does show, for the first time, that the application of higher moment closures to model the initial onset of DDT is technically possible. Furthermore, the work illustrates that two physical limits on the chemical source term closure does in most cases bracket the experimental data. It is also shown that the transported PDF approach can be successfully applied to the modelling of premixed turbulent flames with scalar spaces of sufficient size to model auto-ignition type phenomena. It is also evident from the current work that the modelling of explosion kernels in pre-existing turbulence fields is very sensitive to both the details of the injection process and to the chemical source term closure. The present work does lay the foundations and also indicates the directions for further studies.

Background

Pulsed Detonation Engines (PDEs) cover an unusually wide spectrum of thermochemistry and physics. Examples of physical phenomena of direct relevance to device design include injection and obstacle enhanced localised turbulent explosions resulting in a transition to

REPORT DOCUMENTATION PAGE

Form Approved OMB No. 0704-0188

1. REPORT DATE *(DD-MM-YYYY)* 29-03-2002	2. REPORT TYPE Final Report	3. DATES COVERED *(From – To)* 29 August 2000 - 29-Aug-01

4. TITLE AND SUBTITLE Deflagration to Detonation Transition Processes in Pulsed Detonation Engines	5a. CONTRACT NUMBER F61775-00-WE054
	5b. GRANT NUMBER
	5c. PROGRAM ELEMENT NUMBER
6. AUTHOR(S) Dr. R Peter Lindstedt	5d. PROJECT NUMBER
	5d. TASK NUMBER
	5e. WORK UNIT NUMBER

7. PERFORMING ORGANIZATION NAME(S) AND ADDRESS(ES) Imperial College Consultants Limited (ICON) 47 Prince's Gate Exhibition Road London SW7 2QA United Kingdom	8. PERFORMING ORGANIZATION REPORT NUMBER N/A

9. SPONSORING/MONITORING AGENCY NAME(S) AND ADDRESS(ES) EOARD PSC 802 BOX 14 FPO 09499-0014	10. SPONSOR/MONITOR'S ACRONYM(S)
	11. SPONSOR/MONITOR'S REPORT NUMBER(S) SPC 00-4054

12. DISTRIBUTION/AVAILABILITY STATEMENT

Approved for public release; distribution is unlimited.

13. SUPPLEMENTARY NOTES

14. ABSTRACT

This report results from a contract tasking Imperial College Consultants Limited (ICON) as follows: The contractor will evaluate the use of a closure model with transported pdf approaches closed at the joint scalar and joint velocity-scalar levels. A key advantage here is the potential ability to model kinetically controlled/influenced phenomena such as flame extinction and (auto-) ignition. The latter clearly plays a key role in the onset of DDT. The present proposal thus includes a detailed assessment of such aspects through the gradual introduction of increasingly accurate closure elements under conditions of relevance to PDE devices. The experimental data to be used will feature the unique data sets produced at Imperial College as part of earlier investigations and cover multiple obstacle configurations and the effects of initial turbulence on the evolution of turbulent gaseous explosions. The data sets include time-resolved mean and turbulence velocity measurements, ionization probe data, pressure information and visualization through schlieren photography. The current work will form a direct basis for further consideration of new experimental and theoretical work performed in geometries and under conditions derived in close collaboration with AFRL/PR.

15. SUBJECT TERMS
EOARD, Combustion, Detonation, Pulsed Detonation Engines (PDE)

16. SECURITY CLASSIFICATION OF:			17. LIMITATION OF ABSTRACT UL	18, NUMBER OF PAGES	19a. NAME OF RESPONSIBLE PERSON Wayne Donaldson
a. REPORT UNCLAS	b. ABSTRACT UNCLAS	c. THIS PAGE UNCLAS		38	19b. TELEPHONE NUMBER *(Include area code)* +44 (0)20 7514 4299

Standard Form 298 (Rev. 8/98)
Prescribed by ANSI Std. Z39-18

detonation, the propagation of the resulting detonation and its interaction with confinement boundaries. The resulting flow is of a time-dependent compressible nature in which the chemical structure of the fuel has been shown experimentally to have a leading order influence on the transition process. Furthermore, an exceptionally wide range of turbulence Reynolds numbers is encountered. The suggested topics were identified as key issues during a recent Window on Science (WOS) visit to NASA Glenn Research Centre (GRC) in Cleveland, OH and the Air Force Research Laboratories (AFRL) at Wright Patterson AFB located in Dayton, OH. Significant contributions to the understanding related relevant phenomena have recently been made at Imperial College in the context of repeated UK industrial and EU sponsored projects. The study is theoretical, but has utilised detailed (e.g. including mean and rms velocities) new experimental data covering the effects of initial turbulence and obstacle configurations on the transition process.

Work Programme
The chemistry of a particular fuel and the actual flow conditions play major roles in determining the time and length scales for DDT. The latter parameters, along with high reproducibility, are likely to play a key role in device design. The consequences of such experimental observations for computational design techniques are notable. In particular, the significant differences in techniques applied by the detonation physics community, which tends to deal with shock induced ignition/transition phenomena, and the approaches required to model the onset of detonation in a turbulent medium are profound. A focal point of the current proposal is thus to establish the capabilities of possible computational modelling techniques in the context of DDT under conditions directly relevant to PDEs. The temporal response of turbulent flames and turbulence-kinetic interactions evidently occupy central roles in emerging propulsion devices in general [1] and during the DDT phase of PDEs in particular. However, current computational design techniques, commonly based on eddy viscosity closures coupled with fast-chemistry type approximations, preclude the modelling of direct kinetic effects. Furthermore, even such techniques have not been rigorously assessed against detailed experimental data of relevance to PDEs. At a more fundamental level, significant difficulties relating to qualitatively correct predictions of key features such as flame generated turbulence [2,3] prevail for such closures. A key feature in this context is the need for correct predictions also of parameters related to flame dynamics. The current research programme aims to:

(i)   Provide an assessment of the ability of high Damköhler number approaches combined with eddy viscosity approximations to model qualitatively and quantitatively the evolution of a turbulent gaseous explosion in a confined channel with obstacles and an initially quiescent mixture.

(ii)   Provide an assessment of the ability of high Damköhler number approaches combined with eddy viscosity approximations to model qualitatively and quantitatively the evolution of a turbulent gaseous explosion in a confined channel in the presence of obstacles and a pre-existing turbulence field.

(iii)   Evaluate the potential of improved techniques. Closures at the second moment level are capable of dealing with flame generated turbulence and do provide better flame dynamics provided that the second moment level is utilized for both velocity and scalar fields. Recent developments of closures at this level have lead to their successful application to transient multi-dimensional premixed [2,3,4] and partially premixed flames [4].

(iv)   Evaluate further the potential of the transported *pdf* approach in the context of premixed flames [4,5]. The technique has the particular benefit that chemical reaction is treated in a closed form and key advantage in the present context is thus the potential ability to model kinetically controlled/influenced phenomena such as flame extinction and (auto-) ignition. Due to the computational expense of the approach only idealized geometries can be covered as part of the current work programme.

The experimental data used for tasks (i) to (iii) will feature the unique data sets [6-8] produced at Imperial College as part of earlier investigations. The data sets include time-resolved mean and turbulence velocity measurements, ionization probe data, pressure information and visualization through schlieren photography.

Task 1: Eddy Viscosity Based Modelling of Turbulent Gaseous Explosions in a Confined Channel with an Initially Quiescent Mixture.
The transient interaction of flames with obstacles is a key phenomenon in determining the severity of turbulent gaseous explosions. In the first task the transition of a confined, initially laminar, stoichiometric methane–air flame to a strongly turbulent deflagration caused by its interaction with a baffle-type obstacle has been studied in detail. The time dependent flow characteristics, including velocity vectors and Reynolds stress components, determined by Lindstedt & Sakthitharan [6] in a two-dimensional plane along the vertical tube axis through the use of Laser Doppler Anemometry (LDA), are used. The experimental configurations are explained in Figure 1.

The configuration corresponding to Task 1 yields a significant explosion with an over-pressure close to 100 kPa and peak (mean) flow velocities approaching 100 m/s. Typical RMS velocities are of the order 4 m/s and significant levels of anisotropy are observed in the shear layer above the obstacle. It is shown that for the geometry studied the turbulent rate of strain significantly exceeds the bulk rate of strain. Measurements through the turbulent flame brush also indicate that in the absence of mean velocity gradients the turbulence intensities are unchanged or marginally enhanced by the presence of the flame. The conditions are thus more benign than in a PDE, but the current data set is virtually unique in providing sufficient detail to enable significant progress to be made in the development/validation of models describing the initial turbulent gaseous explosion which subsequently leads to DDT.

The modelling approach taken here is as outlined by Arntzen *et al.* [9] and features a fractal based eddy-breakup model for the turbulent reaction rate. The resulting expression exhibits a scaling based on both integral and Kolmogorv scales as outlined by Lindstedt and Vaos [2].

The solution shown is grid independent and features around 100 000 locally refined computational cells in a two-dimensional geometry. The computations feature a second order TVD scheme and an implicit predictor corrector methods [2].

The computed and measured [6] pressure traces are shown in Figure 2. There has been no translation of the data to account for inaccuracies in the initial (laminar) flame propagation phase. The agreement may be termed satisfactory. In subsequent figures the velocity traces have been translated to align the peaks of measured and computed pressures. Examples of velocity field predictions are given in Figures 3 and 4, where axial (u) and transverse (v) velocity components are compared with measurements using two types of flow seeding. The agreement is, perhaps surprisingly, not unreasonable. However, the anisotropy indicated by the measurements can, naturally, not be reproduced by the eddy-viscosity based closure used for the velocity field. Furthermore, the occurrence of the second peak in velocities is not well reproduced. The implication is that the dynamics of the explosion is accurately represented. Nevertheless, the very rapid changes in the two mean velocity components are well reproduced by the computations as shown in Figures 5 and 6 respectively. Furthermore, the evolution of the rms components, shown in Figures 7 and 8, remains reasonable with the caveats outlined above.

Task 2: Eddy Viscosity Based Modelling of Turbulent Gaseous Explosions in a Confined Channel with Initial Turbulence.
The transition of a turbulent flame to a gaseous explosion in a confined pre-existing turbulent flow field is of more direct practical interest in the current context and a corresponding data set has been produced by Lindstedt & McCann [10]. One obvious and related topic is the intentional transition to detonation in pulsed detonation engines. Experimental data sets suitable for the developments of predictive techniques are naturally required in order to advance the basic understanding of such flows. The present report thus outlines the use of data from the above [10] experimental study into the interactions between baffle accelerated premixed turbulent flames and their self-generated flow in a long flame tube. In particular, the ability of the modelling approach outlined in Task 1 to reproduce the effects of a pre-existing velocity field at the ignition point located upstream of the baffle is examined. Flow characteristics, including time-resolved mean and rms profiles in a two-dimensional plane, obtained using laser Doppler anemometry for a stoichiometric methane-air flame [10] are compared to simulation results. The present configuration yields over-pressures of around 200 kPa and peak mean velocities around 200 m/s – both significantly higher than those reported by Lindstedt & Sakthitharan [6] for initially quiescent mixtures. In addition the turbulence velocities reach values of the order 40 m/s.

In the initial study, computations have been performed with two types of initial conditions. In the first set the measured jet velocity profile was used as the basis for the imposition of a similarity solution based initial condition. In the second set of calculations the flow in the geometry was solved, including the initial jet, to generate a more complete initial flow field description prior to ignition. The results are exemplified in Figures 9 and 10. The two cases

differ significantly and there are also notable differences with the measured jet profiles. The effects upon the computed pressure profiles are shown in Figure 11. The most notable discrepancy is clearly with respect to the computed peak pressure. The measured profile shows a higher peak pressure followed by a more rapid decline. It would appear evident that the dynamics of the explosion is captured less well for the case with initial turbulence. However, it is also evident that the initial conditions have a significant bearing on the outcome of the computations.

Comparisons of velocity profiles are also illuminating. The initial rise in the axial velocity is comparatively well reproduced as shown in Figure 12. However, the second velocity peak resulting from the explosion in the pocket behind the obstacle is notably absent. Furthermore, while turbulence intensities are reasonably well reproduced close to the obstacle, as shown in Figures 13 and 14, the complicated dual peaks arising further downstream are not as well predicted as shown in Figure 15. Furthermore, it is notable that despite the under-prediction in over-pressure, the actual turbulence intensities are over-predicted and thus indicate errors in the temporal evolution of the explosion. Nevertheless, given that the current computations feature a very stern test and that model parameters have not been changed to enhance agreement with experimental data, the results may be termed encouraging and the effects of improved closures for the velocity and scalar fields are explored in Task 3.

Task 3: Second Moment Based Modelling of Turbulent Gaseous Explosions in a Confined Channel.

Work has been completed successfully also on this task and the computational results reported constitute the first successful application of second moment based calculation procedures to model turbulent gaseous explosions. The second moment closure applied corresponds to that of Lindstedt & Vaos [2] without the implementation of the preferential acceleration terms. The applied closure does, however, include the scalar fluxes and the computational grid (~ 100 000 nodes) is identical to the previous computations. Two separate closures for the chemical source term have been included. The first features the standard eddy breakup model with a presumed bimodal variance and the second a fractal flame surface area based modification identical to that applied in Tasks 1 and 2. A discussion on the topic has been provided by Lindstedt & Vaos [2] and is not repeated here. The standard eddy break up closure results form the assumption of an inner cutoff of the fractal dimension corresponding to the Gibson scale. The resulting expression is equivalent to the intuitively derived eddy break model of Spalding. The closure omits all chemical and structural limitations on the chemical source term and the results obtained therefore represent an upper limit on the heat release rate. The fractal expression is based on the assumption of an inner cutoff of the fractal dimension corresponding to the Kolmogorov scales. The resulting expression yields a reduction in the heat release through the introduction of the ratio of the laminar burning velocity to the Kolmogorov velocity. The expression has been found to work exceptionally well for cases of low turbulence where the inherent laminar flamelet assumption is valid. The two cases may be viewed as limiting. The initial conditions used correspond to results from the imposed similarity solution discussed in Task 2.

The predicted pressure traces obtained with the two models are shown in Figure 16. The initial conditions are identical in both cases. It is interesting to note that it would indeed appear that the experimental traces are bracketed by the two computations. Further evidence that the predictions are qualitatively good and quantitatively reasonable can be found in predictions of the axial and cross stream mean velocities shown in Figures 17 and 18. It is here important to point out that the exceptionally strong acceleration shown in the computations would be exceptionally difficult to capture experimentally and it is likely that the measurements underestimate the second peak in the axial velocity shown in Figure 17. The further observation that the second peak is predicted well qualitatively is important. The same peak is notably absent in the eddy viscosity simulation shown in Figure 12. It is very interesting to note that the improved closure for turbulent transport does improve predictions considerably. The strong effect of the chemical source term closure (and hence the heat release rate) is perhaps most evident in Figure 18. A further observation that is perhaps surprisingly encouraging is that the computed turbulence levels are comparatively well reproduced up to the point of the explosion as shown in Figure 19. Furthermore, the calculation appears to predict broadly the right level of (strong) anisotropy in the shear layer above the obstacle. None of these effects are reproduced by the eddy viscosity computations.

Similar observations can be made further downstream form the obstacle at the 515 mm plane as shown in Figures 20 to 24. A particularly interesting feature is the predicted high level of axial and cross-stream turbulence and the fact that the axial component is not picked up the experimental data while the cross-stream component evidently is. Given that it can be expected that the axial component is greater, it would appear possible that the flow acceleration has been too strong for the LDA seeding particles to follow.

Task 4: Further Evaluation of the Potential of Transported PDF Approaches in the Context of Premixed Turbulent Flames.
Combustion chemistry and kinetically controlled effects have traditionally been of secondary concern in the design of propulsion devices. However, the apparent need to deal with fuel effects and turbulence chemistry interactions, as highlighted above, is now becoming evident. The transported PDF approach uniquely offers the advantage of facilitating the inclusion of direct kinetic effects in a closed form. In the present work, transported PDF computations, closed at the joint-scalar level, have been performed for high velocity, high Reynolds number, jet flames using comprehensive chemistry and a second moment closure for the velocity field. The solution method for the joint-scalar PDF equation features moving particles in a Lagrangian framework and micro-mixing processes are modelled using the standard smooth kernel variation of Curl's model. The systematically reduced chemistry stems from the recent work of Lindstedt and co-workers [12] and features up to 12 independent scalars solved through direct integration. The application of a rigorous systematic reduction procedure has shown that the remaining species can be considered in steady-state under all conditions of relevance to the present study.

Of particular interest to the present study is the ability to assess the modelling of finite rate chemistry effects associated with phenomena such as heat release and thus CO to CO2 conversion. The application of chemical kinetics to the design and analysis of propulsion devices has traditionally been limited to features that may be treated as perturbations on solutions obtained with infinite rate (equilibrium) chemistry. A typical example is the computation of nitric oxide emissions from gas turbine combustors obtained via the use of a conserved scalar, presumed β-PDF approach coupled with the Zel'dovich (thermal) nitric oxide formation mechanism. The relative success of this approach[1] is readily shown to be strongly dependent upon the burning mode of traditional gas turbine combustors and the associated high temperatures and pressures. The usefulness of approaches of the type outlined above may often be somewhat extended through the application of laminar flamelet based techniques. However, the treatment of direct kinetic effects must still proceed through a similar perturbation approach. Such computations have to date featured the application of global, rather than systematically reduced, mechanisms due to the inherent complexity of the soot formation process. Further improvements may be obtained though the use of conditional moment or time-dependent flamelet closures as discussed below. However, it may also be shown that design computations exhibit a strong sensitivity to flow field predictions as well as to kinetic parameters. Additional complications may be expected in supersonic/ hypersonic devices [1]. For example, the composition of cracked products from endothermic fuels may be expected to significantly influence the operational characteristics of burners. Ignition delay times can also be expected to significantly depend on the actual reactant composition delivered.

The increasing need for energy efficient low-emission combustion technologies is also resulting in significant changes in the operating conditions of practical burners. A direct consequence of current developments is that combustion devices are increasingly affected by complex interactions between turbulence and finite rate chemistry. Typical examples of such interactions include the occurrence of (partial) flame extinction and re-ignition due to aerodynamic strain and the formation of major pollutants. Traditional moment-method based approaches impose considerable limitations on how such effects can be incorporated into practical calculation procedures. Furthermore, the applicability of resulting models is almost without exception confined to specific types of flames/combustion regimes and/or favourable operating envelopes. By contrast, transported probability density function (PDF) based methods provide a rigorous framework wherein finite rate chemistry effects are directly incorporated in a closed form. In the context of transported pdf methods closed at the joint-scalar level, major closure elements include conditional velocity and molecular flux terms in the PDF equation, terms which essentially represent turbulent transport effects in physical and scalar spaces respectively. In the present work a transported PDF approach, closed at the joint scalar level, is applied to the simulation of a range of premixed turbulent flames. The second order closure by Speziale et al. is used for the velocity field and a gradient diffusion type model is adopted for the closure of the transport of the PDF in physical space. Molecular micro-mixing processes are represented by the smooth kernel variation of Curl's particle interaction model.
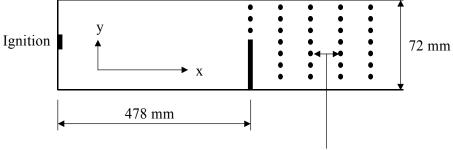
Work has reached a conclusion also on this task and computations have been performed for an idealised geometry featuring the highly turbulent flames stabilised on a Bunsen burner and as investigated experimentally by Chen *et al.* [11]. The computations have been performed with, for the first time in the context of premixed turbulent flames, comprehensive chemistry. The approach is thus similar to that applied by Lindstedt *et al.* [12] for the modelling of turbulent jet diffusion flames. Predictions of key properties are reproduced with surprising accuracy as can be seen in Figures 16 to 20. The results obtained are interesting and show, arguably for the first time, that transported PDF approaches can reproduce detailed high Reynolds number flame data for premixed flames with good accuracy. It is appears evident that the transported PDF approach holds significant promise also for premixed turbulent flames at the high Reynolds numbers which may be expected as part of the DDT process [6,10]. The conclusion is important given the strong influence of the chemical source term upon the rate of heat release in the current application area. A further key point is that fuel effects – of key importance in practice – are incorporated naturally into the approach.

Deviations from Workplan
There have been no major technical deviations from the initial work plan. However, the use of a joint velocity scalar closure has been replaced by the use of accurate large scalar space chemistry following the apparent success of this approach in diffusion flames [12] and the evident importance of the closure for the chemical reaction source term. Progress was initially slow due to staffing difficulties. The interim report was, as a result, issued late and an additional delay was encountered due to further personnel changes. However, the work progressed well since the appointment of a new student.

References

[1] Tishkoff, J.M., Drummond, J.P., Edwards, T. and Nejad, A.S. 'Future Direction of Supersonic Combustion Research: Air Force/NASA Workshop on Supersonic Combustion', AIAA 97-1017 (1997).

[2] Lindstedt, R.P. and Vaos, E.M. 'Modelling of Premixed Turbulent Flames with Second Moment Methods', *Combustion and Flame* 116, (1999), pp. 461-485.

[3] Lindstedt, R.P. and Vaos, E.M. 'Second Moment Modelling of Premixed Turbulent Flames Stabilised in Impinging Jet Geometries', *Twenty-Seventh Symposium (International) on Combustion/The Combustion Institute*, Pittsburgh, (1998), pp. 957-962.

[4] Hulek, T. "Modelling of Turbulent Combustion using Transported Probability Density Function Methods Methods." *Ph.D. Thesis*, University of London, 1996.

[5] Hulek, T. and Lindstedt, R.P. 'Computations of Steady-State and Transient Premixed Turbulent Flames using Transported *pdf* Methods', *Combustion and Flame*, 104, (1996), pp. 481-504.

[6] Lindstedt, R.P. and Sakthitharan, V., "Time Resolved Velocity and Turbulence Measurements in Turbulent Gaseous Explosions", *Combustion and Flame*, 114 (1998) pp. 469-483.

[7] Sakthitharan, V. "Time-Resolved Measurements of Flame Propagation over Baffle-Type Obstacles", Ph.D. Thesis, Imperial College, 1995.

[8] McCann, H.A. "Time Resolved Measurements of Propagating Turbulent Flames", Ph.D. Thesis, Imperial College, 1997.

[9] Arntzen, B.J., Hjertager, B., Lindstedt, R.P., Mercx, W.P.M. and Popat, N. "Investigations to Improve and Assess the Accuracy of Computational Fluid Dynamic Based Explosion Models", *Journal of Hazardous Materials*, 45, (1995) pp. 1-25.

[10] Lindstedt, R.P. and McCann, H.A. "Time Resolved Flow Characteristics of Confined Turbulent Gaseous Explosions", Presented at the 18th ICDRS Meeting Seattle, August 2001.

[11] Chen, Y.-C., Peters, N., Schneeman, G.A., Wruck, N., Renz, U. and Mansour, M.S. "Detailed Flame Structures of Highly Stretched Turbulent Premixed Methane-Air Flames", *Combustion and Flame* 107, (1996) pp. 223-244.

[12] Lindstedt, R.P., Loloudi, S.A. and Vaos, E.M. "Joint Scalar Probability Density Function Modeling of Pollutant Formation in Piloted Turbulent Jet Diffusion Flames with Comprehensive Chemistry", *Proceedings of the Combustion Institute*, 28:149-156 (2000).

Figure 1. Experimental layout for the case without initial turbulence [6] using a coarse measurement matrix. The full measurement matrix features a separation of 25 mm in the horizontal direction and additional points above the obstacle. For the case with initial turbulence a central jet is placed at the right hand side boundary and the obstacle is located at the 415 mm plane. The channel is 11 m in length.
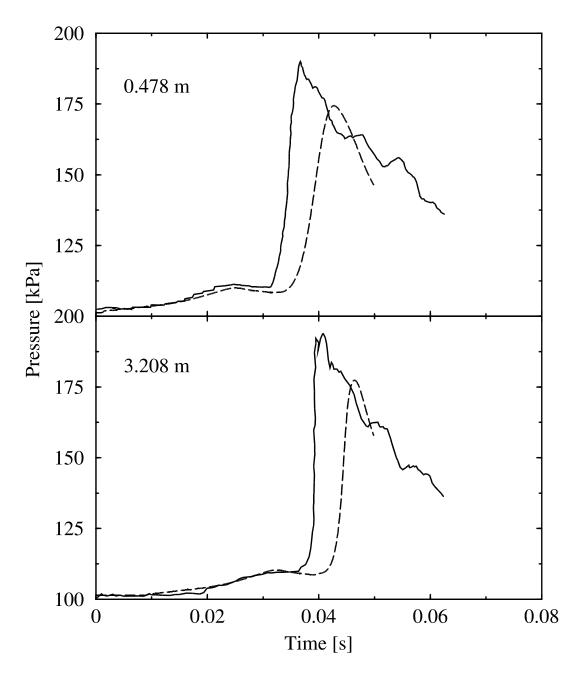
Figure 2. Comparison of computed and measured [6] pressure traces for a turbulent gaseous explosion in an initially quiescent mixture at two axial locations along the explosion tube.
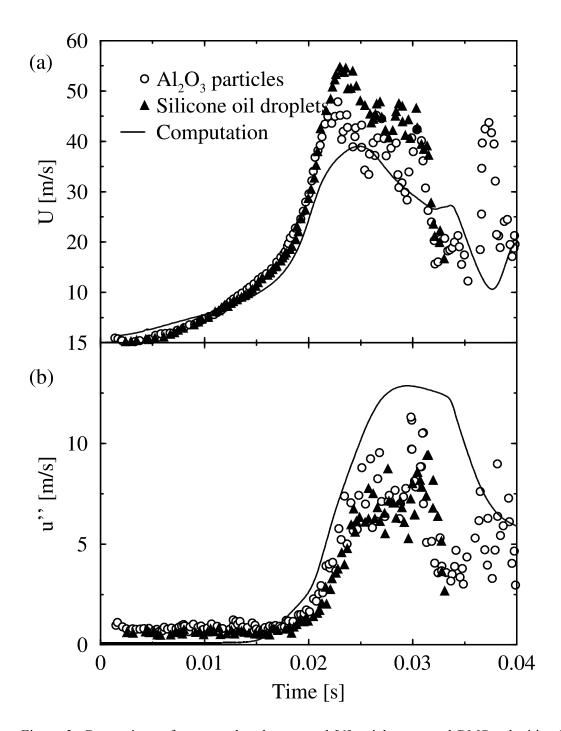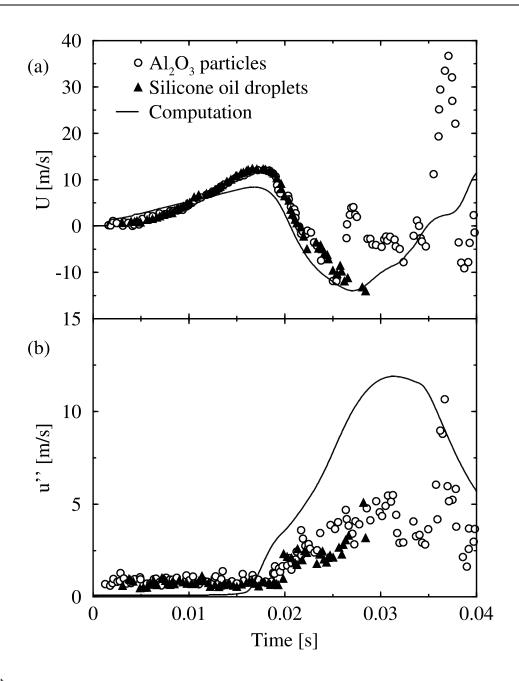
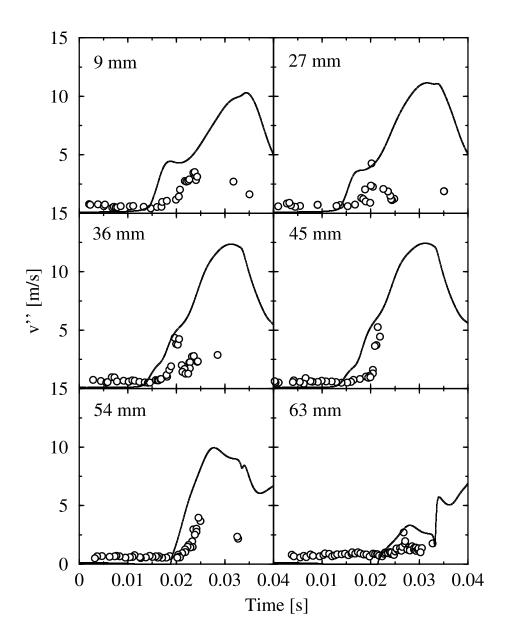Figure 3. Comparison of computed and measured [6] axial mean and RMS velocities for a turbulent gaseous explosion in an initially quiescent mixture. Experimental results obtained with two types of flow seeding are used for comparison purposes and the measurement location is at the 578 mm plane and 45 mm from the bottom wall.

Figure 4. Comparison of computed and measured [6] cross-stream mean and RMS velocities for a turbulent gaseous explosion in an initially quiescent mixture. Experimental results obtained with two types of flow seeding are used for comparison purposes and the measurement location is at the 578 mm plane and 18 mm from the bottom wall.
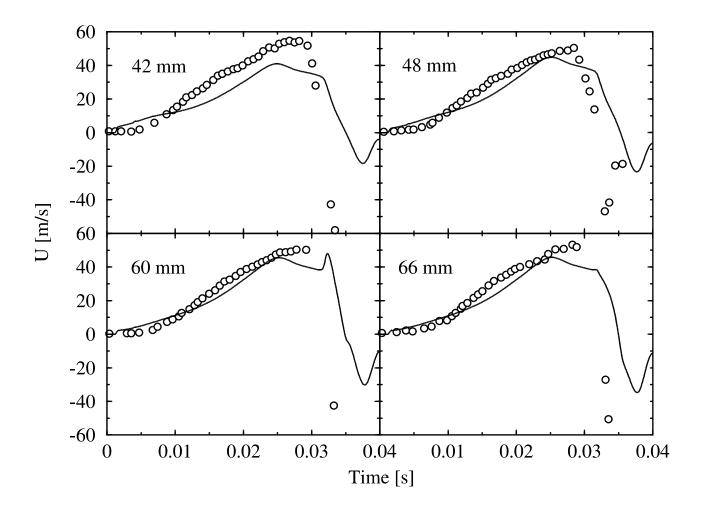
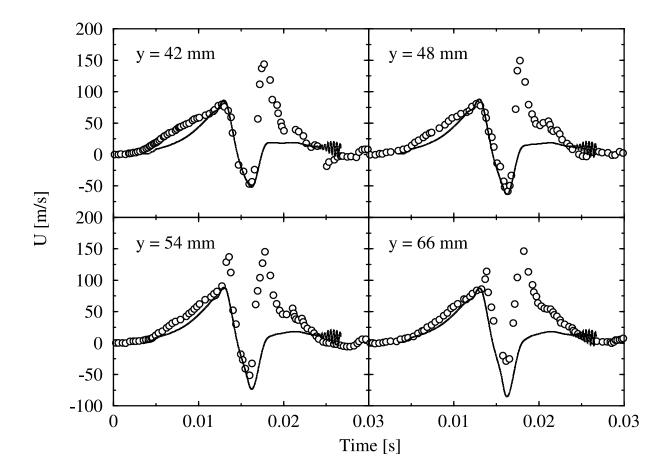Figure 5. Comparison of computed and measured [6] axial mean velocities along the 478 mm plane (directly above the obstacle) for a turbulent gaseous explosion in an initially quiescent mixture.
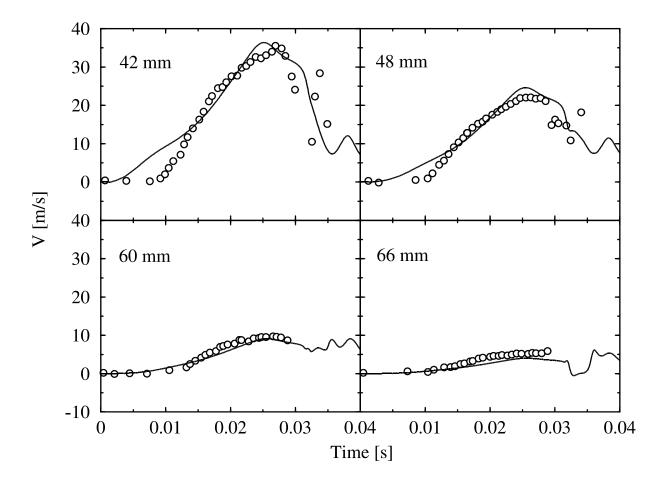
Figure 6. Comparison of computed and measured [6] cross-stream mean velocities along the 478 mm plane (directly above the obstacle) for a turbulent gaseous explosion in an initially quiescent mixture.
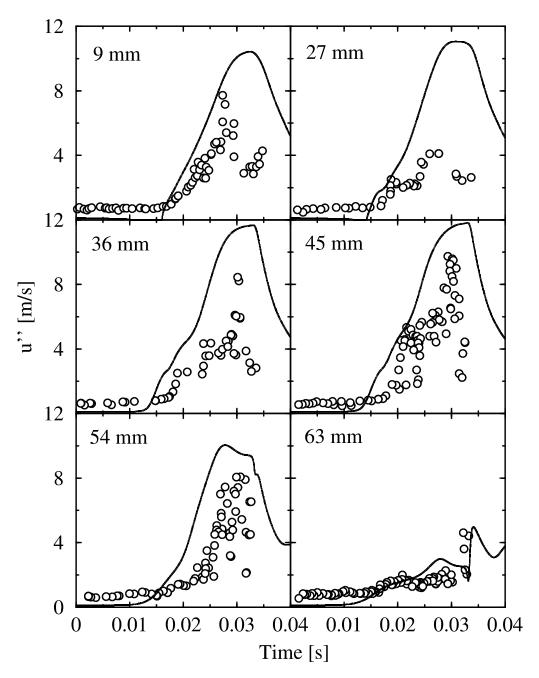
Figure 7. Comparison of computed and measured [6] axial RMS velocities along the 553 mm plane for a turbulent gaseous explosion in an initially quiescent mixture.

Figure 8. Comparison of computed and measured [6] cross-stream RMS velocities along the $y = 53$ mm plane for a turbulent gaseous explosion in an initially quiescent mixture.
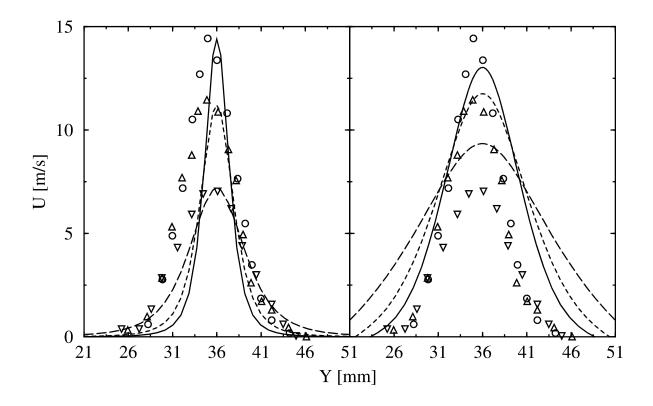
Figure 9. Comparison of computed and measured [9] axial mean velocities at 3 measuring stations (27, 37 and 62 mm) along the initial jet for a turbulent gaseous explosion in a pre-existing turbulence field. The graph on the left indicates the similarity based initial condition and the graph on the right the solution obtained by the use of an eddy viscosity based model.
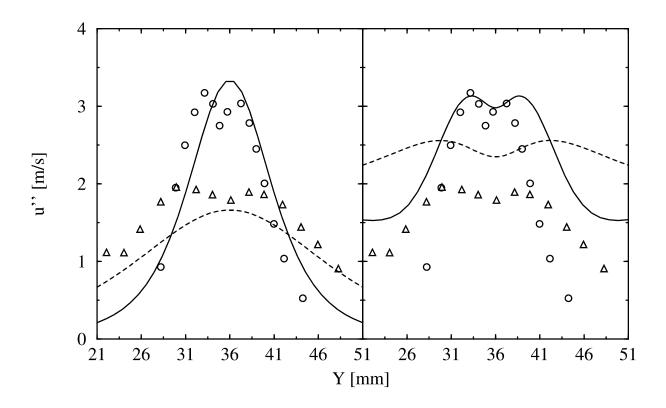
Figure 10. Comparison of computed and measured [9] axial RMS velocities at 2 measuring stations (27 and 62 mm) along the initial jet for a turbulent gaseous explosion in a pre-existing turbulence field. The graph on the left indicates the similarity based initial condition and the graph on the right the solution obtained by the use of an eddy viscosity based model.
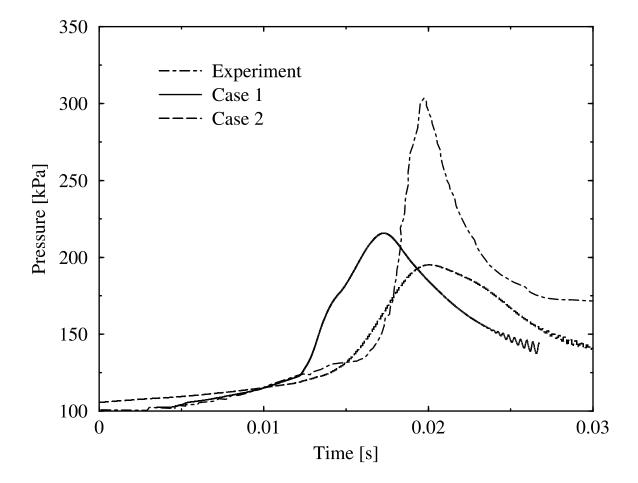
Figure 11. Comparison of computed and measured [9] pressure traces for a turbulent gaseous explosion in a pre-existing turbulence field. Case 1 indicates the solution obtained by the use of an eddy viscosity based model and Case 2 the similarity based initial condition.
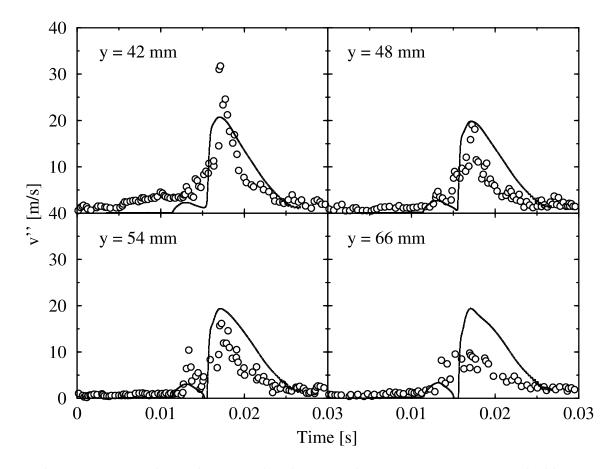
Figure 12. Comparison of computed and measured [9] axial mean velocities at 4 measuring stations along the 415 mm plane (directly above the obstacle) for a turbulent gaseous explosion in a pre-existing turbulence field. The graph shows the solution obtained by the use of an eddy viscosity based model.
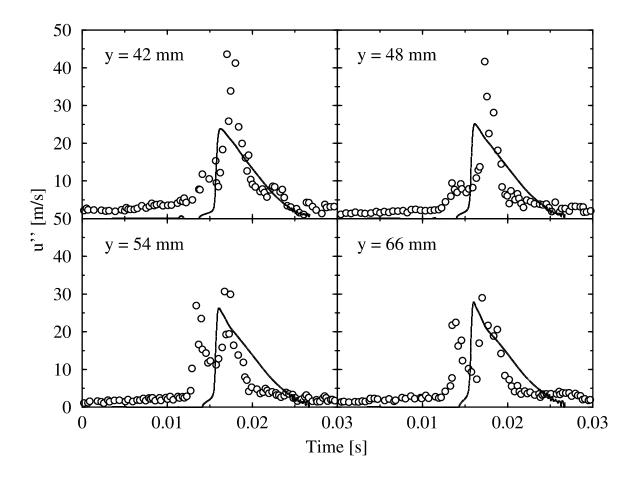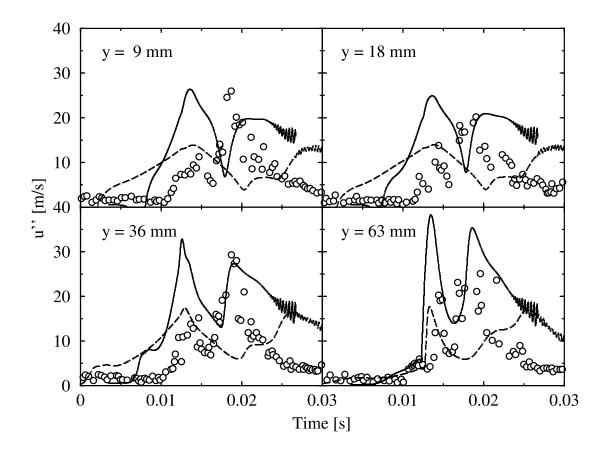
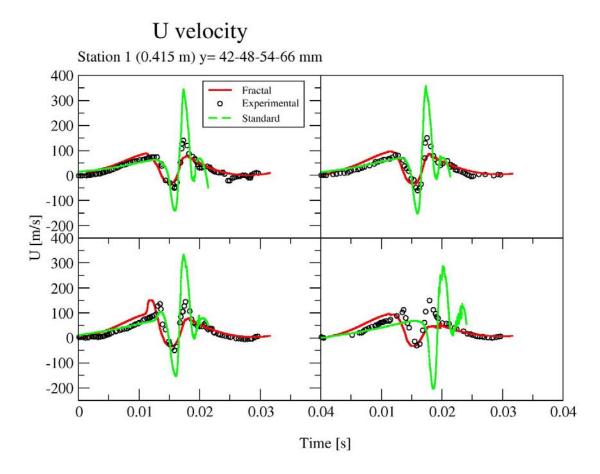Figure 13. Comparison of computed and measured [9] axial RMS velocities at 4 measuring stations along the 415 mm plane (directly above the obstacle) for a turbulent gaseous explosion in a pre-existing turbulence field. The graph shows the solution obtained by the use of an eddy viscosity based model.

Figure 14. Comparison of computed and measured [9] cross-stream RMS velocities at 4 measuring stations along the 415 mm plane (directly above the obstacle) for a turbulent gaseous explosion in a pre-existing turbulence field. The graph shows the solution obtained by the use of an eddy viscosity based model.

Figure 15. Comparison of computed and measured [9] axial RMS velocities at 4 measuring stations along the 515 mm plane (100 mm away from the obstacle) for a turbulent gaseous explosion in a pre-existing turbulence field. The solid line shows the solution obtained by the use of an eddy viscosity based model and the dashed line the solution resulting from the imposed similarity solution.
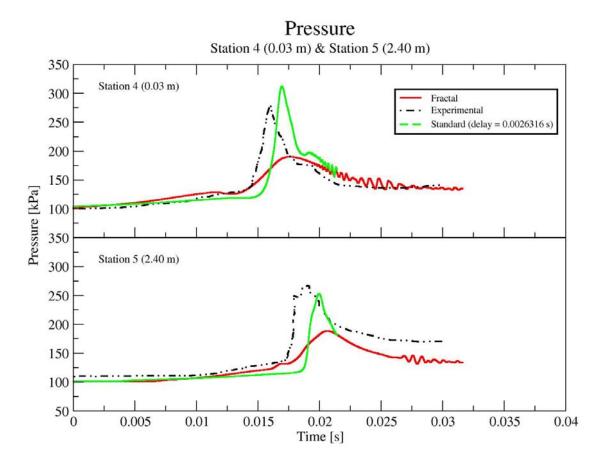
Figure 16. Comparison of computed and measured [9] pressure traces for a turbulent gaseous explosion in a pre-existing turbulence field. The initial conditions correspond to results from the imposed similarity solution. The dashed lined indicates the use of the eddy break up closure with an inner cut-off for the fractal dimension on the Gibson scale and the solid line an inner cut-off on the Kolmogorov scale.

Figure 17. Comparison of computed and measured [9] axial mean velocities at 4 measuring stations along the 415 mm plane (directly above the obstacle) for a turbulent gaseous explosion in a pre-existing turbulence field. The graph shows the solution obtained by the use of a second moment closure for both the velocity and scalar fields. The dashed lined indicates the use of the eddy break up closure with an inner cut-off for the fractal dimension on the Gibson scale and the solid line an inner cut-off on the Kolmogorov scale.
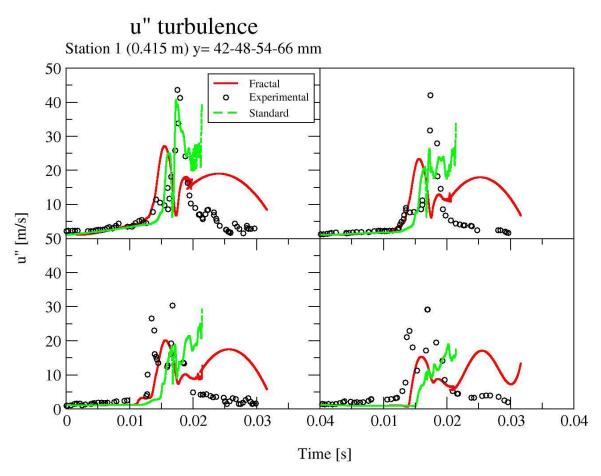
V velocity

Station 1 (0.415 m) y= 42-48-54-66 mm

Figure 18. Comparison of computed and measured [9] cross-stream mean velocities at 4 measuring stations along the 415 mm plane (directly above the obstacle) for a turbulent gaseous explosion in a pre-existing turbulence field. The graph shows the solution obtained by the use of a second moment closure for both the velocity and scalar fields. The dashed lined indicates the use of the eddy break up closure with an inner cut-off for the fractal dimension on the Gibson scale and the solid line an inner cut-off on the Kolmogorov scale.
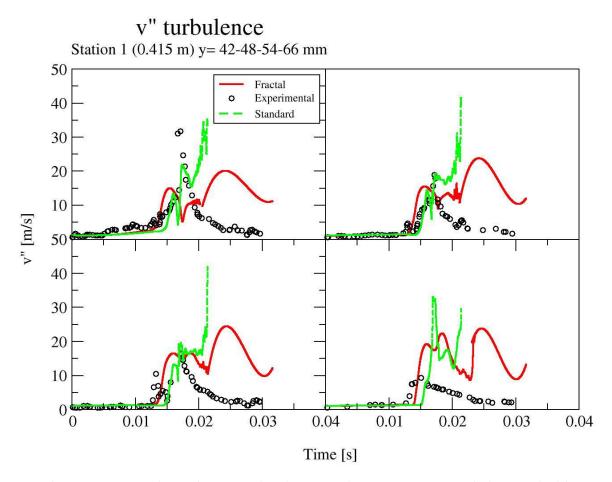
Figure 19. Comparison of computed and measured [9] axial turbulence velocities at 4 measuring stations along the 415 mm plane (directly above the obstacle) for a turbulent gaseous explosion in a pre-existing turbulence field. The graph shows the solution obtained by the use of a second moment closure for both the velocity and scalar fields. The dashed lined indicates the use of the eddy break up closure with an inner cut-off for the fractal dimension on the Gibson scale and the solid line an inner cut-off on the Kolmogorov scale.
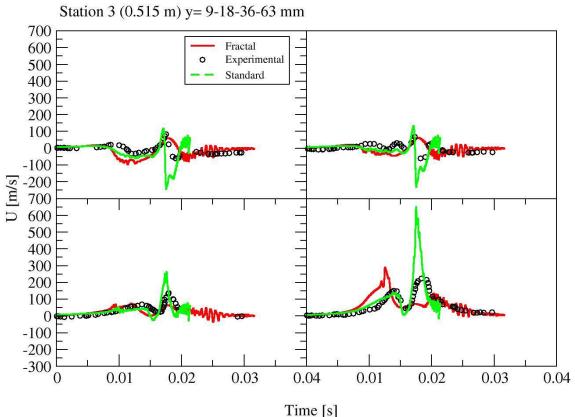
v" turbulence
Station 1 (0.415 m) y= 42-48-54-66 mm

Figure 20. Comparison of computed and measured [9] cross stream turbulence velocities at 4 measuring stations along the 415 mm plane (directly above the obstacle) for a turbulent gaseous explosion in a pre-existing turbulence field. The graph shows the solution obtained by the use of a second moment closure for both the velocity and scalar fields. The dashed lined indicates the use of the eddy break up closure with an inner cut-off for the fractal dimension on the Gibson scale and the solid line an inner cut-off on the Kolmogorov scale.
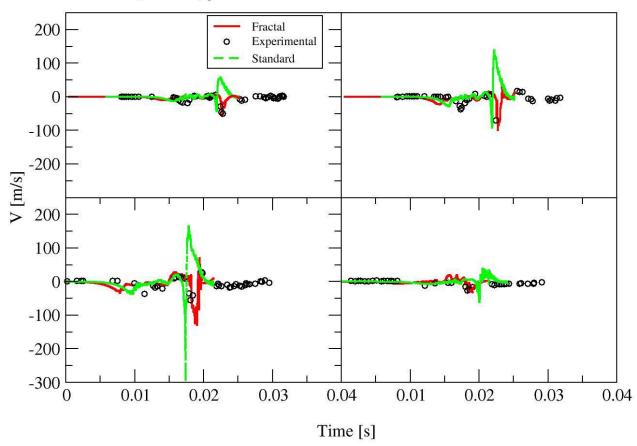
Figure 21. Comparison of computed and measured [9] axial mean velocities at 4 measuring stations along the 515 mm plane (100 mm away from the obstacle) for a turbulent gaseous explosion in a pre-existing turbulence field. The initial conditions correspond to results from the imposed similarity solution. The dashed lined indicates the use of the eddy break up closure with an inner cut-off for the fractal dimension on the Gibson scale and the solid line an inner cut-off on the Kolmogorov scale.

Figure 22. Comparison of computed and measured [9] cross stream mean velocities at 4 measuring stations along the 515 mm plane (100 mm away from the obstacle) for a turbulent gaseous explosion in a pre-existing turbulence field. The initial conditions correspond to results from the imposed similarity solution. The dashed lined indicates the use of the eddy break up closure with an inner cut-off for the fractal dimension on the Gibson scale and the solid line an inner cut-off on the Kolmogorov scale.

Figure 23. Comparison of computed and measured [9] axial turbulence velocities at 4 measuring stations along the 515 mm plane (100 mm away from the obstacle) for a turbulent gaseous explosion in a pre-existing turbulence field. The initial conditions correspond to results from the imposed similarity solution. The dashed lined indicates the use of the eddy break up closure with an inner cut-off for the fractal dimension on the Gibson scale and the solid line an inner cut-off on the Kolmogorov scale.

Figure 24. Comparison of computed and measured [9] cross stream turbulence velocities at 4 measuring stations along the 515 mm plane (100 mm away from the obstacle) for a turbulent gaseous explosion in a pre-existing turbulence field. The initial conditions correspond to results from the imposed similarity solution. The dashed lined indicates the use of the eddy break up closure with an inner cut-off for the fractal dimension on the Gibson scale and the solid line an inner cut-off on the Kolmogorov scale.
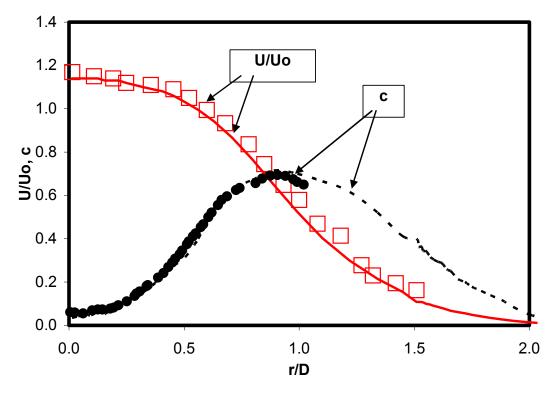
Figure 25. Comparisons of measurements [11] and computations of normalized axial mean velocity and reaction progress variable (c) at a down stream location of x/d = 8.5. A time scale ratio of 2 is used in the simulation.
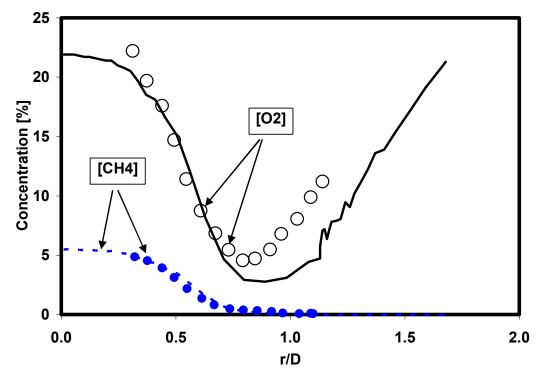
Figure 26. Comparisons of measurements [11] and computations of fuel and oxygen concentrations at a down stream location of x/d = 4.5. A time scale ratio of 2 is used in the simulation.
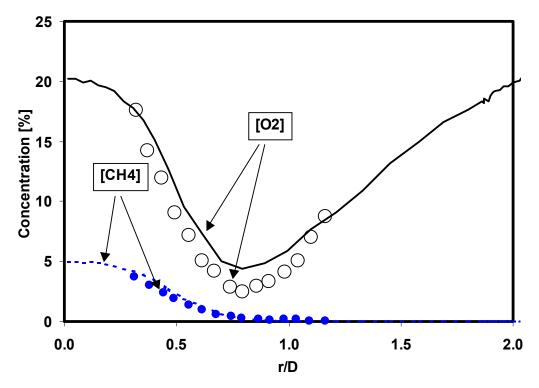
Figure 27. Comparisons of measurements [11] and computations of fuel and oxygen concentrations at a down stream location of x/d = 8.5. A time scale ratio of 4 is used in the simulation.
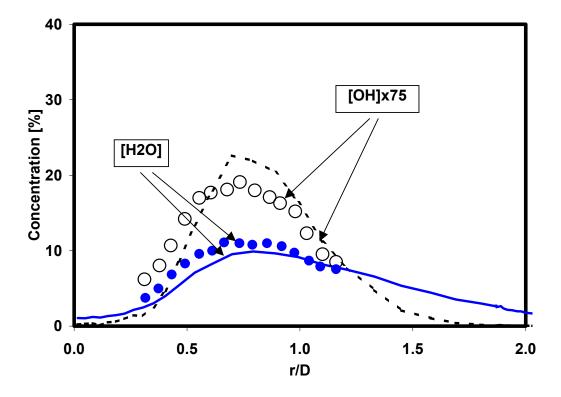
Figure 28. Comparisons of measurements [11] and computations of water and OH radical concentrations at a downstream location of x/d = 8.5. A time scale ratio of 2 is used in the simulation.
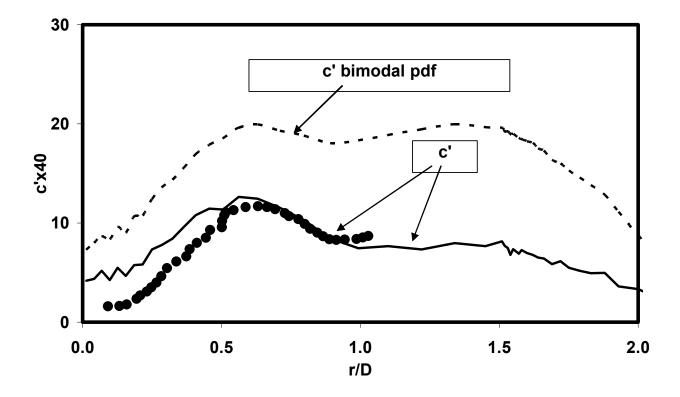
Figure 29. Comparisons of measurements [11] and computations of reaction variable fluctuations at a downstream location of x/d = 8.5. A time scale ratio of 2 is used in the simulation and the result obtained through the use of a bimodal approximation is also shown.